

# BIFURCATION AND COMPARISON OF A DISCRETE-TIME HINDMARSH-ROSE MODEL

Yue Li<sup>1</sup> and Hongjun Cao<sup>1,†</sup>

**Abstract** In this paper, a Hindmarsh-Rose model discretized by a nonstandard finite difference (NSFD) scheme is considered. Bifurcation behaviors are compared between the model obtained by the forward Euler scheme and the model obtained by the NSFD scheme. Through analytical and numerical comparisons, the Neimark-Sacker bifurcation of the model discretized by the NSFD method is closer to the Hopf bifurcation of the original continuous Hindmarsh-Rose model than that discretized by the forward Euler method. Moreover, due to the NSFD method's better stability and convergence, the integral step size can be chosen larger in the NSFD scheme. And much more dynamic behaviors can be obtained by using the NSFD scheme than those in the forward Euler scheme. These confirmed results can at least guarantee true available numerical results to investigate complex neuron dynamical systems.

**Keywords** Nonstandard finite difference scheme, discrete-time Hindmarsh-Rose model, stability, fold bifurcation, Neimark-Sacker bifurcation.

**MSC(2010)** 34, 37.

## 1. Introduction

Many dynamical systems are represented by nonlinear differential equations whose analytical solutions are usually hard to obtain. Under this circumstance, how to take into account the dynamical behaviors of these nonlinear differential equations effectively is of great significance.

Among so many methods to deal with the above problem, the discretization is a straightforward way. There are several ways to transform a continuous differential system into a corresponding discrete mapping. The most commonly used method for this aim is the standard difference methods, such as the forward Euler scheme, the Runge-Kutta method and so on. Nevertheless, there have been so many unclear questions so far. The key point is how to preserve the basic structures and main properties of the original continuous dynamical system after discretization as much as possible. In particular, the numerical instabilities should be considered before the implementation of standard finite difference schemes.

To eliminate numerical instabilities, the NSFD schemes have been proposed by many researchers, for example like [15] and therein. In addition, dynamic consistency must be considered, which is also a goal for proposing the NSFD methods. A difference equation is called dynamically consistent with the differential equation if they both possess the same dynamics such as stability, bifurcation, and chaos [2].

<sup>†</sup>The corresponding author. Email: [hjcao@bjtu.edu.cn](mailto:hjcao@bjtu.edu.cn)(H.J. Cao)

<sup>1</sup>Mathematics, School of Science, Beijing Jiaotong University, Beijing 100044, China

The main advantage of NSFD schemes can retain the considerable properties of their original continuous systems to guarantee true numerical results. While the construction of these NSFD schemes is not easy, because there is no general criterion for construction.

Over the past decades, there have been numerous interesting results from using the NSFD method. Some results also proved that the stability and convergence of the NSFD methods are better than some standard difference schemes. For example, in [6], authors developed positive and elementary stable nonstandard (PESN) finite-difference methods for predator-prey systems. They found that the PESN methods keep both the positivity of the solutions and the stability of the equilibria of the corresponding predator-prey system. A NSFD scheme that was constructed to simulate a predator-prey model of Gause-type with a functional response is consistent with the asymptotic dynamics of the model. It was also compared with those obtained from the standard methods such as the forward Euler and the Runge-Kutta methods [16]. Other applications and analyses of the NSFD scheme can be found in [1, 3, 5, 10, 17]. Moreover, Mickens's method was generalized by Roeger. Simultaneously, a class of nonstandard symplectic numerical methods for a Lotka-Volterra system was given [19]. Roeger et al. constructed a discrete Lotka-Volterra competition model by applying the NSFD schemes. It proved the dynamic consistency between the resulting difference equation and the differential equation [20]. Kahan et al. presented an unconventional method with second-order accuracy [9]. Roeger used conformal mappings to study the relationship between the eigenvalues of the Jacobian matrices of the differential equations and the resulting difference equations. He proved that Kahan's discretization method preserves the local stability and the Hopf bifurcation of any fixed points while Euler's method fails. Unfortunately, Kahan's method can only be applied to the differential equation  $\frac{dx}{dt} = f(x)$  where  $f(x)$  is at most quadratic in  $x$  [21].

So it is worth discretizing a neuron model with cubic terms and studying its dynamic behavior by using a kind of NSFD method. A classical Hindmarsh-Rose neuron model [22] with cubic terms is chosen in this paper as follows:

$$\begin{cases} \frac{dx}{dt} = c \left( x - \frac{x^3}{3} - y + I \right), \\ \frac{dy}{dt} = \frac{x^2 + dx - by + a}{c}. \end{cases} \quad (1.1)$$

Herein,  $x$  represents the membrane potential,  $y$  is an internal or recovery variable,  $I$  is the stimulus intensity and  $a, b, c, d$  are all positive parameters.

There are several reasons for choosing this model:

(i). Hindmarsh-Rose model is a classical neuron model and has been widely studied.

Many researchers have used the bifurcation theory to study the complex dynamics of the Hindmarsh-Rose model. In [23], the authors proposed two Hindmarsh-Rose neurons with the same synaptic coupling and discussed how coupling strength and time delay affect dynamics by studying the stabilities and bifurcations at equilibria. Some conclusions could be regarded as theoretical guidance for the study of the dynamics of coupled neurons.

(ii). There have been many works on the discretization of the Hindmarsh-Rose model.

The forward Euler scheme is the more frequently used method to discretize a Hindmarsh-Rose model. Yu and Cao [25] discretized a three-dimensional Hindmarsh-

Rose model by the forward Euler scheme and then investigated the existence of one-parameter bifurcations in the discrete model. They illustrated the correctness of the bifurcation analysis by numerical computation. Li and He [14] proved that a two-dimensional discrete Hindmarsh-Rose model can produce two kinds of codimension-one bifurcations (flip bifurcation, Neimark-Sacker bifurcation) and a codimension-two bifurcation (1:1 resonance). In addition, they also carried out numerical computations, which illustrated the theoretical results and showed some complex dynamic behaviors. Felicio and Rech [7] presented a two-dimensional parameter-plane diagram for a three-dimensional discrete Hindmarsh-Rose model. Moreover, periodic structures can be observed clearly in a two-dimensional parameter-plane diagram. Kuznetsov and Sedova [11] analyzed the quasi-periodic bifurcations of a map by observing two-dimensional parameter-plane diagrams corresponding to different integral step sizes.

(iii). The model (1.1) is a relatively simple two-dimensional Hindmarsh-Rose model with cubic terms, which made the implementation of theoretical analysis and calculation less complicated and relatively feasible.

Besides, Li and He [13] studied the dynamic properties like periodic structures and bifurcation types of the model which is obtained by applying the forward Euler scheme to discretize the model (1.1):

$$\begin{pmatrix} x \\ y \end{pmatrix} \mapsto \begin{pmatrix} x + hc \left( x - \frac{x^3}{3} - y + I \right) \\ y + \frac{h}{c} (x^2 + dx - by + a) \end{pmatrix}, \quad (1.2)$$

where  $h$  is the step size. This paper mainly focus on the comparison of bifurcations between the model (1.2) and the model discretized by the NSFD method.

In this paper, a NSFD scheme is applied to the model (1.1) and the following discrete-time model is obtained:

$$\begin{pmatrix} x \\ y \end{pmatrix} \mapsto \begin{pmatrix} \frac{6h(x-2y)c^2 + ((3b-3d)x-6a)h^2 + 12x)c + 6bhx}{4ch^2\left(\frac{dx^3}{2} + \left(a + \frac{3}{2} - \frac{by}{2}\right)x^2 - \frac{3xy}{2} + \frac{3}{4}y(b-d) - \frac{3a}{2}\right) + ((4x^2y-6y)c^2 - 6by + 12(dx+x^2+a))h + 12cy}{M} \end{pmatrix}, \quad (1.3)$$

where  $M = (4x^2 - 6)hc^2 + (12 + (2bx^2 - 3b + 3d + 6x)h^2)c + 6bh$ . The detailed calculation is in Appendix A. In order to guarantee the model is meaningful, suppose  $M \neq 0$ . Assume that  $I = 0$  in this paper [4].

Unlike most implicit discrete schemes which cannot be solved explicitly, one of the novelties of this paper is that the explicit expressions can be solved in this paper as equation (1.3), which facilitates our research. The goal is to compare the difference between the model obtained by the forward Euler scheme and the discrete-time Hindmarsh-Rose model obtained by the NSFD scheme. For the sake of simplicity in the computation, the projection method is used to calculate the normal forms of one-parameter bifurcations at the fixed points of the model (1.3). Based on the bifurcation analysis, several behaviors for the two-dimensional Hindmarsh-Rose model are simulated and compared near bifurcation points. When the step size  $h$  is the same, the bifurcation parameter of the Hopf bifurcation of the model (1.3) obtained by the NSFD method is closer to the original continuous model than the model (1.2) obtained by the forward Euler method. In addition, because of the better stability and convergence of the NSFD method, when the step size increases, the difference equation still converges and more dynamic phenomena can

be obtained such as the chaotic attractor, which is demonstrated by numerical simulation.

The layout of this paper is as follows. In section 2, from the point of view of qualitative and quantitative analysis for bifurcation, the existence and stability of the fixed points for model (1.3) are concerned, which makes the bifurcation analysis more accurate and the corresponding comparison more specific, especially in numerical simulation. In section 3, sufficient conditions for fold bifurcation and Neimark-Sacker bifurcation at fixed points of model (1.3) are given and the differences on bifurcations between model (1.2) and model (1.3) are discussed. The theoretical results are identified by numerical simulation in section 4, where complex dynamics like periodic structures, invariant closed orbits and chaotic attractor are observed. Moreover, the results of numerical simulation of the forward Euler scheme and the NSFD scheme are compared, especially in two-dimensional parameter-plane diagrams. Finally, conclusions are given in section 5.

## 2. Existence and Stability of fixed points of the model (1.3)

The existence and stability of the fixed points of the model (1.3) are analyzed, which provides a precondition for the analysis and comparison of the bifurcation and facilitates the selection of parameters in numerical simulation.

### 2.1. Existence

For model (1.1), the equilibria should satisfy the following conditions

$$\begin{cases} \frac{b}{3}x^3 + x^2 + (d-b)x + a = 0, \\ y = x - \frac{x^3}{3}. \end{cases} \quad (2.1)$$

In the same way, the fixed points  $E(x, y)$  of the model (1.3) satisfy the following equations

$$\begin{cases} \frac{6h(x-2y)c^2 + ((3b-3d)x-6a)h^2 + 12x)c + 6bhx}{M} = x, \\ \frac{4ch^2(\frac{dx^3}{2} + (a + \frac{3}{2} - \frac{by}{2})x^2 - \frac{3xy}{2} + \frac{3}{4}y(b-d) - \frac{3a}{2}) + ((4x^2y-6y)c^2 - 6by + 12(dx+x^2+a)h + 12cy)}{M} = y. \end{cases} \quad (2.2)$$

Then we have

$$\begin{cases} (\frac{bx^3}{3} + x^2 + (d-b)x + a)h + \frac{2c}{3}(x^3 - 3x + 3y) = 0, \\ ch(\frac{dx^3}{2} + (a - by + \frac{3}{2})x^2 - 3xy + \frac{3}{2}((b-d)y - a)) + 3(a - by + dx + x^2) = 0. \end{cases} \quad (2.3)$$

Through variable transformations, we get the following conditions for the fixed points of the model (1.3),

$$\begin{cases} \frac{b}{3}x^3 + x^2 + (d-b)x + a = 0, \\ y' = -\frac{(bh+2c)x^3}{6c} - \frac{hx^2}{2c} - \frac{(-3bh+3dh-6c)x}{6c} - \frac{ah}{2c}. \end{cases} \quad (2.4)$$

Note that when the equation  $\frac{b}{3}x^3 + x^2 + (d-b)x + a = 0$  holds,  $y' - y = 0$ . So the equilibria of model (1.1) is also the fixed points of model (1.3). Here we only study the equilibria that retained after discretization.

## 2.2. Stability

The Jacobian matrix  $J(x_k, y_k)$  of the model (1.3) evaluated at one of the above fixed points at  $E_k(x_k, y_k)$  is given by

$$J(x_k, y_k) = \begin{pmatrix} J_{11} & J_{12} \\ J_{21} & J_{22} \end{pmatrix}, \quad (2.5)$$

where the expression of  $J_{11}$ ,  $J_{12}$ ,  $J_{21}$ ,  $J_{22}$  are given in the Appendix B.

The corresponding characteristic equation can be written as

$$h(\lambda) = \lambda^2 - (Ba + C)\lambda + (Da + E) = 0. \quad (2.6)$$

It is easy to obtain the eigenvalues

$$\lambda_{1,2} = \frac{Ba + C}{2} \pm \frac{\sqrt{\Delta}}{2},$$

where  $\Delta = (Ba + C)^2 - 4(Da + E)$ , and the the expression of  $B$ ,  $C$ ,  $D$ ,  $E$  are presented in the Appendix C.

### Proposition 2.1.

(i) The fixed point  $E_k$  of model (1.3) is a stable focus if one of the following conditions holds:

$$\begin{aligned} (a) \quad & \frac{-BC+2D-2\sqrt{B^2E-BCD+D^2}}{B^2} < a < \frac{-BC+2D+2\sqrt{B^2E-BCD+D^2}}{B^2}, \quad a < \frac{1-E}{D} \quad (D > 0); \\ (b) \quad & \frac{-BC+2D-2\sqrt{B^2E-BCD+D^2}}{B^2} < a < \frac{-BC+2D+2\sqrt{B^2E-BCD+D^2}}{B^2}, \quad a > \frac{1-E}{D} \quad (D < 0). \end{aligned}$$

(ii) The fixed point  $E_k$  of model (1.3) is an unstable focus if one of the following conditions satisfies:

$$\begin{aligned} (a) \quad & \frac{-BC+2D-2\sqrt{B^2E-BCD+D^2}}{B^2} < a < \frac{-BC+2D+2\sqrt{B^2E-BCD+D^2}}{B^2}, \quad a > \frac{1-E}{D} \quad (D > 0); \\ (b) \quad & \frac{-BC+2D-2\sqrt{B^2E-BCD+D^2}}{B^2} < a < \frac{-BC+2D+2\sqrt{B^2E-BCD+D^2}}{B^2}, \quad a < \frac{1-E}{D} \quad (D < 0). \end{aligned}$$

### Proposition 2.2.

(i) The fixed point  $E_k$  of model (1.3) is an unstable source if one of the following conditions holds:

$$\begin{aligned} (a) \quad & -a \geq \frac{2D-BC+2\sqrt{B^2E-BCD+D^2}}{B^2} \quad \text{or} \quad a \leq \frac{2D-BC-2\sqrt{B^2E-BCD+D^2}}{B^2}, \\ & a < \frac{1+E-C}{B-D} \quad (B-D < 0), \quad a < \frac{-1-E-C}{B+D} \quad (B+D > 0); \\ (b) \quad & -a \geq \frac{2D-BC+2\sqrt{B^2E-BCD+D^2}}{B^2} \quad \text{or} \quad a \leq \frac{2D-BC-2\sqrt{B^2E-BCD+D^2}}{B^2}, \\ & a < \frac{1+E-C}{B-D} \quad (B-D < 0), \quad a > \frac{-1-E-C}{B+D} \quad (B+D < 0); \\ (c) \quad & -a \geq \frac{2D-BC+2\sqrt{B^2E-BCD+D^2}}{B^2} \quad \text{or} \quad a \leq \frac{2D-BC-2\sqrt{B^2E-BCD+D^2}}{B^2}, \\ & a > \frac{1+E-C}{B-D} \quad (B-D > 0), \quad a < \frac{-1-E-C}{B+D} \quad (B+D > 0); \end{aligned}$$

- (d)  $-a \geq \frac{2D-BC+2\sqrt{B^2E-BCD+D^2}}{B^2}$  or  $a \leq \frac{2D-BC-2\sqrt{B^2E-BCD+D^2}}{B^2}$ ,  
 $a > \frac{1+E-C}{B-D}(B-D > 0)$ ,  $a > \frac{-1-E-C}{B+D}(B+D < 0)$ ;
- (e)  $-a \geq \frac{2D-BC+2\sqrt{B^2E-BCD+D^2}}{B^2}$  or  $a \leq \frac{2D-BC-2\sqrt{B^2E-BCD+D^2}}{B^2}$ ,  
 $a < -\frac{C+2}{B}(B > 0)$ ,  $a < \frac{-1-E-C}{B+D}(B+D < 0)$ ;
- (f)  $-a \geq \frac{2D-BC+2\sqrt{B^2E-BCD+D^2}}{B^2}$  or  $a \leq \frac{2D-BC-2\sqrt{B^2E-BCD+D^2}}{B^2}$ ,  
 $a < -\frac{C+2}{B}(B > 0)$ ,  $a > \frac{-1-E-C}{B+D}(B+D > 0)$ ;
- (g)  $-a \geq \frac{2D-BC+2\sqrt{B^2E-BCD+D^2}}{B^2}$  or  $a \leq \frac{2D-BC-2\sqrt{B^2E-BCD+D^2}}{B^2}$ ,  
 $a > -\frac{C+2}{B}(B < 0)$ ,  $a < \frac{-1-E-C}{B+D}(B+D < 0)$ ;
- (h)  $-a \geq \frac{2D-BC+2\sqrt{B^2E-BCD+D^2}}{B^2}$  or  $a \leq \frac{2D-BC-2\sqrt{B^2E-BCD+D^2}}{B^2}$ ,  
 $a > -\frac{C+2}{B}(B < 0)$ ,  $a > \frac{-1-E-C}{B+D}(B+D > 0)$ ;
- (i)  $-a \geq \frac{2D-BC+2\sqrt{B^2E-BCD+D^2}}{B^2}$  or  $a \leq \frac{2D-BC-2\sqrt{B^2E-BCD+D^2}}{B^2}$ ,  
 $a > -\frac{C+2}{B}(B > 0)$ ,  $a < \frac{1+E-C}{B-D}(B-D > 0)$ ;
- (j)  $-a \geq \frac{2D-BC+2\sqrt{B^2E-BCD+D^2}}{B^2}$  or  $a \leq \frac{2D-BC-2\sqrt{B^2E-BCD+D^2}}{B^2}$ ,  
 $a > -\frac{C+2}{B}(B > 0)$ ,  $a > \frac{1+E-C}{B-D}(B-D < 0)$ ;
- (k)  $-a \geq \frac{2D-BC+2\sqrt{B^2E-BCD+D^2}}{B^2}$  or  $a \leq \frac{2D-BC-2\sqrt{B^2E-BCD+D^2}}{B^2}$ ,  
 $a > -\frac{C+2}{B}(B < 0)$ ,  $a < \frac{1+E-C}{B-D}(B-D > 0)$ ;
- (l)  $-a \geq \frac{2D-BC+2\sqrt{B^2E-BCD+D^2}}{B^2}$  or  $a \leq \frac{2D-BC-2\sqrt{B^2E-BCD+D^2}}{B^2}$ ,  
 $a > -\frac{C+2}{B}(B < 0)$ ,  $a > \frac{1+E-C}{B-D}(B-D < 0)$ .

(ii) The fixed point  $E_k$  of model (3) is a saddle if one of the following conditions holds:

- (a)  $a \geq \frac{2D-BC+2\sqrt{B^2E-BCD+D^2}}{B^2}$  or  $a \leq \frac{2D-BC-2\sqrt{B^2E-BCD+D^2}}{B^2}$ ,  
 $\frac{-BC+D+\sqrt{(E+1)^2B^2-2BCD+D^2}(C^2-E^2-2E)}{B^2-D^2}$   
 $< a < \frac{-BC+D-\sqrt{(E+1)^2B^2-2BCD+D^2}(C^2-E^2-2E)}{B^2-D^2} (D^2 - B^2 > 0)$ ;
- (b)  $a \geq \frac{2D-BC+2\sqrt{B^2E-BCD+D^2}}{B^2}$  or  $a \leq \frac{2D-BC-2\sqrt{B^2E-BCD+D^2}}{B^2}$ ,  
 $a < \frac{-BC+D-\sqrt{(E+1)^2B^2-2BCD+D^2}(C^2-E^2-2E)}{B^2-D^2}$   
or  $a > \frac{-BC+D+\sqrt{(E+1)^2B^2-2BCD+D^2}(C^2-E^2-2E)}{B^2-D^2} (D^2 - B^2 < 0)$ .

The proofs of the above two propositions are presented in the Appendix D.

**Remark 2.1.** The fixed point satisfying the above conditions does not necessarily exist. The parameters selected in section 4 (numerical simulations) are all satisfied with the existence conditions of the fixed points.

**Remark 2.2.** From the above two propositions, it can be seen that the stability of the fixed points is related to the step size  $h$ . So the size of the discrete step  $h$  must be considered in the discrete model.

### 3. Bifurcation Analysis

This section mainly focuses on the one-parameter bifurcations of the model (1.3) which is investigated by the projection method [12]. More importantly, the comparison of bifurcations between model (1.2) and model (1.3) is discussed.

Let  $u = x - x_k$  and  $v = y - y_k$ , then we transform  $E_k(x_k, y_k)$  to the origin. By introducing a new variable  $X = (u, v)^T$  ( $(\cdot)^T$  denotes the transpose of  $(\cdot)$ ), model (1.3) can be transformed into the form

$$X \mapsto G(X), \quad (3.1)$$

where  $G = (G_1, G_2)^T$  with

$$\begin{aligned} G_1 &= \frac{6hc^2(u-2v-x_k+2y_k)+((3(b-d)(u-x_k)-6a)h^2+12(u-x_k)c+6bh(u-x_k))}{4hc^2(u^2-2ux_k+x_k^2-\frac{3}{2})+(12+(2bu^2+(6-4bx_k)u+2bx_k^2+3(d-b)-6x_k)h^2)c+6bh}, \\ G_2 &= \frac{4((4(v-y_k)(u^2-2ux_k+x_k^2-\frac{3}{2})c^2+12(u^2+(d-2x_k)u)+6b(y_k-v)+12(x_k^2-dx_k+a)h+12c(v-y_k))}{4hc^2(u^2-2ux_k+x_k^2-\frac{3}{2})+(12+((2u^2-4ux_k+2x_k^2-3)b+3d+6u-6x_k)h^2)c+6bh} \\ &\quad - \frac{ch^2(2dx_k^2+2x_k^2(b(y_k-v)+3)+6x_k(v-y_k)3v(b-d)+3y_k(d-b)-6a)}{4hc^2(u^2-2ux_k+x_k^2-\frac{3}{2})+(12+((2u^2-4ux_k+2x_k^2-3)b+3d+6u-6x_k)h^2)c+6bh} \\ &\quad + \frac{4ch^2(\frac{du^3+(b(y_k-v)-3dx_k+3+2a)u^2}{2}+(\frac{3dx_k^2}{2}+(b(v-y_k)-2a-3)x_k+\frac{3(y_k-v)}{2})u)}{4hc^2(u^2-2ux_k+x_k^2-\frac{3}{2})+(12+((2u^2-4ux_k+2x_k^2-3)b+3d+6u-6x_k)h^2)c+6bh}. \end{aligned}$$

For model (3.1), we obtain

$$X \mapsto JX + \frac{1}{2}B(X, X) + \frac{1}{6}C(X, X, X) + O(|X|^4), \quad (3.2)$$

and let

$$F(X) = \frac{1}{2}B(X, X) + \frac{1}{6}C(X, X, X) + O(|X|^4),$$

where  $J = J(E_k)$  and  $B(X, X)$  and  $C(X, X, X)$  are multilinear functions with

$$B(x, y) = \sum_{i,j=1}^2 \left. \frac{\partial^2 F(\xi)}{\partial \xi_i \partial \xi_j} \right|_{\xi=0} x_i y_j = \begin{pmatrix} b_1 \\ b_2 \end{pmatrix} x_1 y_1 + \begin{pmatrix} b_3 \\ b_4 \end{pmatrix} (x_1 y_2 + x_2 y_1),$$

and

$$\begin{aligned} C(x, y, w) &= \sum_{i,j,l=1}^2 \left. \frac{\partial^3 F(\xi)}{\partial \xi_i \partial \xi_j \partial \xi_l} \right|_{\xi=0} x_i y_j w_l \\ &= \begin{pmatrix} c_1 \\ c_2 \end{pmatrix} x_1 y_1 w_1 + \begin{pmatrix} c_3 \\ c_4 \end{pmatrix} (x_1 y_1 w_2 + x_1 y_2 w_1 + x_2 y_1 w_1), \end{aligned}$$

where the expression of  $b_1, b_2, b_3, b_4$  and  $c_1, c_2, c_3, c_4$  are given in the Appendix E.

#### 3.1. Fold bifurcation

In the following analysis of the fold bifurcation, parameter  $a$  is chosen as the bifurcation parameter. Bifurcation analysis for the models (1.1), (1.2), and (1.3) is performed by the bifurcation theory at  $E_k(x_k, y_k)$ , which is more convenient to make a comparison of bifurcation between these three models.

First, the characteristic polynomial corresponding to the Jacobian matrix at the fixed point  $E_k(x_k, y_k)$  of the model (1.1) is

$$H(\lambda) = \lambda^2 - \left( -cx_k^2 + c - \frac{b}{c} \right) \lambda + bx_k^2 + 2x_k - b + d.$$

A fold bifurcation may occur at the fixed point  $E_k(x_k, y_k)$  if the following conditions are satisfied [12]:

$$\begin{cases} H(0) = bx_k^2 + 2x_k - b + d = 0, \\ \frac{b}{3}x_k^3 + x_k^2 + (d - b)x_k + a = 0. \end{cases}$$

It is easy to conclude that when  $a = \frac{(-1 \pm \sqrt{b^2 - bd + 1})(2b^2 - 2bd + 1 \mp \sqrt{b^2 - bd + 1})}{3b^2}$ , there exists a fold bifurcation at the fixed point  $E_k(x_k, y_k)$ , where  $x_k = \frac{-1 \pm \sqrt{b^2 - bd + 1}}{b}$ ,  $y_k = x_k - \frac{x_k^3}{3}$ .

Next, the characteristic polynomial of the Jacobian matrix at the fixed point  $E_k(x_k, y_k)$  of the model (1.2) is

$$P(\lambda) = \lambda^2 + \left( \left( cx_k^2 - c + \frac{b}{c} \right) h - 2 \right) \lambda + (bx_k^2 + 2x_k - b + d) h^2 - \left( cx_k^2 - c + \frac{b}{c} \right) h + 1.$$

Like the analysis of the model (1.1), if the following conditions are satisfied, model (1.2) may undergo a fold bifurcation at the fixed point  $E_k(x_k, y_k)$  [12]:

$$\begin{cases} P(1) = (bx_k^2 + 2x_k - b + d) h^2 = 0, \\ \frac{b}{3}x_k^3 + x_k^2 + (d - b)x_k + a = 0. \end{cases}$$

It means that a fold bifurcation may occur at the fixed point  $E_k(x_k, y_k)$  when  $a = \frac{(-1 \pm \sqrt{b^2 - bd + 1})(2b^2 - 2bd + 1 \mp \sqrt{b^2 - bd + 1})}{3b^2}$ , where  $x_k = \frac{-1 \pm \sqrt{b^2 - bd + 1}}{b}$ ,  $y_k = x_k - \frac{x_k^3}{3}$ .

For model (1.3), the characteristic polynomial corresponding to the Jacobian matrix at the fixed point  $E_k(x_k, y_k)$  of the model (1.3) is

$$h(\lambda) = \lambda^2 - p(a)\lambda + q(a),$$

where  $p(a) = Ba + C$ ,  $q(a) = Da + E$ .

There exists a fold bifurcation at the fixed point  $E_k(x_k, y_k)$  if the following conditions hold:

$$\begin{cases} h(1) = 1 - p(a) + q(a) = 0, \\ \frac{b}{3}x_k^3 + x_k^2 + (d - b)x_k + a = 0. \end{cases}$$

Thus, when  $a = a_0 = \frac{(-1 \pm \sqrt{b^2 - bd + 1})(2b^2 - 2bd + 1 \mp \sqrt{b^2 - bd + 1})}{3b^2}$ , a fold bifurcation may occur at the fixed point  $E_k(x_k, y_k)$ , where  $x_k = \frac{-1 \pm \sqrt{b^2 - bd + 1}}{b}$ ,  $y_k = x_k - \frac{x_k^3}{3}$ .

It is easy to find that the conditions of the fold bifurcation for these three models are consistent.

Using the corresponding theorems in [8, 12, 24], we obtain the following result of the model (1.3).

**Theorem 3.1.** *If  $\left| \frac{BE-CD+D}{B-D} \right| \neq 1$  and  $\tilde{a}(a_0) \neq 0$ , then model (1.3) undergoes a fold bifurcation at  $E_k(x_k, y_k)$  when  $a = a_0$ . Moreover, if  $\tilde{a}(a_0) < 0$  (resp.,  $\tilde{a}(a_0) > 0$ ), there are two fixed points for  $a < a_0$  (resp.,  $a > a_0$ ). These two fixed points collide at  $a = a_0$ , and disappear when  $a > a_0$  (resp.,  $a < a_0$ ).*

**Proof.** The model (1.3) undergoes a fold bifurcation at the fixed point  $E_k(x_k, y_k)$  as the parameter  $a$  varies in a small neighborhood of  $a_0$ . There exists a critical eigenvalue  $\lambda_1 = 1$ . And supposing that  $|\lambda_2| = \left| \frac{BE-CD+D}{B-D} \right| \neq 1, B - D \neq 0$  are satisfied. There exist  $p_1, q_1 \in R^2$  such that  $J(a_0, x_k, y_k)q_1 = q_1$  and  $J^T(a_0, x_k, y_k)p_1 = p_1$ , where  $J^T(a_0, x_k, y_k)$  is the transpose matrix of  $J(a_0, x_k, y_k)$ .

It is easy to obtain

$$q_1 \sim (q_1^*, 1)^T, p_1 \sim (p_1^*, 1)^T,$$

where “ $\sim$ ” is used for proportional vectors and

$$q_1^* = \frac{2bx_k + 3}{x_k^2 + 2dx_k + 3}, p_1^* = \frac{-(hc(bx_k^2 + \frac{3}{2}(d-b) + 3x_k) + 3b)}{3c^2}.$$

For satisfying the normalization  $\langle p_1, q_1 \rangle = 1$ , where  $\langle p_1, q_1 \rangle = p_1^*q_1^* + p_2^*q_2^* = p_1^*q_1^* + 1$  is the scalar product in  $R^2$ , we choose

$$q_1 = (q_1^*, 1)^T, p_1 = \kappa_1(p_1^*, 1)^T,$$

where

$$\kappa_1 = \frac{1}{p_1^*q_1^* + 1}.$$

Through a series of transformations based on the theorems deduced by Kuznetsov [12], the restriction of the model (3.1) to its one-dimensional center manifold at the critical parameter value  $a_0$  can be transformed into the normal form

$$\eta \mapsto \eta + \tilde{a}(a_0)\eta^2 + \tilde{b}(a_0)\eta^3 + O(\eta^4),$$

where

$$\begin{aligned} \tilde{a}(a_0) &= \frac{1}{2} \langle p_1, B(q_1, q_1) \rangle, \\ \tilde{b}(a_0) &= \frac{1}{6} \left( \langle p_1, C(q_1, q_1, q_1) \rangle - 3 \langle p_1, B(q_1, (J(a_0) - I_2)^{INV} a') \rangle \right), \\ a' &= B(q_1, q_1) - \langle p_1, B(q_1, q_1) \rangle q_1, \end{aligned}$$

which determines the direction of fold bifurcation at the fixed point  $E_k(x_k, y_k)$ , where  $I_2$  is the unit  $2 \times 2$  matrix. In the fold case, the matrix  $(J(a_0) - I_2)$  is noninvertible in  $R^2$ , since  $\lambda_1 = 1$  is the eigenvalue of  $J(a_0)$ . Let  $T^{su}$  denotes a one-dimensional linear eigenspace of  $J(a_0)$  corresponding to all eigenvalues other than  $\lambda_1$ . Notice that  $a' \in T^{su}$ , since  $\langle p_1, a' \rangle = 0$ . The restriction of the linear transformation corresponding to  $J(a_0)$  to its invariant subspace  $T^{su}$  is invertible. Thus, to facilitate the following calculation, we use  $(J(a_0) - I_2)^{INV}$  to denote the inverse of  $(J(a_0) - I_2)$ , where  $INV$  means the inverse in  $T^{su}$ .  $[(J(a_0) - I_2)^{INV} a']$  can be computed by solving the following system

$$\begin{pmatrix} J(a_0) - I_2 & q_1 \\ p_1^T & 0 \end{pmatrix} \begin{pmatrix} (J(a_0) - I_2)^{INV} a' \\ \eta \end{pmatrix} = \begin{pmatrix} a' \\ 0 \end{pmatrix}$$

for  $(J(a_0) - I_2)^{INV} a' \in R^2$  and  $\eta \in R^1$ . Here  $q_1$  and  $p_1$  are the above-defined and normalized eigenvectors of  $J(a_0)$  and  $J^T(a_0)$ , respectively. The  $3 \times 3$  matrix of this system is nonsingular [12].  $\square$

### 3.2. Neimark-Sacker bifurcation

As the fold bifurcation analyzed above, a Neimark-Sacker bifurcation will be studied in this section, the parameter  $a$  is chosen as the bifurcation parameter and bifurcation analysis is performed by bifurcation theory at the fixed point  $E_k(x_k, y_k)$ .

For model (1.1), if the following conditions are satisfied, a Hopf bifurcation may occur at the fixed point  $E_k(x_k, y_k)$ :

$$\begin{cases} \text{trace} = (1 - x^2)c^2 - b = 0, \\ \frac{b}{3}x^3 + x^2 + (d - b)x + a = 0, \end{cases}$$

where the ‘‘trace’’ represents the trace of the Jacobian matrix of the model (1.1) at the fixed point  $E_k(x_k, y_k)$ .

It is easy to know from the above conditions that the model (1.1) may take place a Neimark-Sacker bifurcation at the fixed point  $E_k(x_k, y_k)$  when

$$a = a_1 = \frac{\pm ((2b - 3d)c^2 + b^2) \sqrt{c^2 - b} - 3c^3 + 3bc}{3c^3},$$

where  $x_k = \pm \frac{\sqrt{c^2 - b}}{c}$ ,  $y_k = x_k - \frac{x_k^3}{3}$ .

Similarly, a Neimark-Sacker bifurcation may arise at the fixed point  $E_k(x_k, y_k)$  of the model (1.2), if the following conditions hold:

$$\begin{cases} (1 - x_k^2) c^2 + (bx_k^2 - b + d + 2x_k) hc - b = 0, \\ \frac{b}{3}x_k^3 + x_k^2 + (d - b)x_k + a = 0. \end{cases}$$

Thus, when  $a = a_2$ , a Neimark-Sacker bifurcation may occur at the fixed point  $E_k(x_k, y_k)$ , where

$$\begin{aligned} a_2 &= \frac{(3d - 2b)c^3 + (4b^2h - 5bdh + 3h)c^2 + ((2h^2d - 1)b^2 - (2b^3 + b)h^2 - 3c\sqrt{(c^3 - 2h(b - \frac{d}{2})c^2 + ((b^2 - bd + 1)h^2 - b)c + b^2h)c})}{3c^2(hb - c)^3} \\ &\quad \times \frac{(hc - \sqrt{(c^3 - 2h(b - \frac{d}{2})c^2 + ((b^2 - bd + 1)h^2 - b)c + b^2h)c})}{3c^2(hb - c)^3} - \frac{bh(b^2 + \sqrt{(c^3 - 2h(b - \frac{d}{2})c^2 + ((b^2 - bd + 1)h^2 - b)c + b^2h)c})}{3c^2(hb - c)^3}, \\ x_k &= \frac{-hc \pm \sqrt{(c^3 - 2h(b - \frac{d}{2})c^2 + ((b^2 - bd + 1)h^2 - b)c + b^2h)c}}{c(bh - c)}, y_k = x_k - \frac{x_k^3}{3}. \end{aligned}$$

As the study of the model (1.1) and the model (1.2), a Neimark-Sacker bifurcation may undergo at the fixed point  $E_k(x_k, y_k)$  of the model (1.3) if the following conditions are satisfied:

$$\begin{cases} q(a) = 1, \\ \frac{b}{3}x_k^3 + x_k^2 + (d - b)x_k + a = 0. \end{cases}$$

It means that when  $a = a_3$ , a Neimark-Sacker bifurcation may occur at the fixed point  $E_k(x_k, y_k)$ , where

$$a_3 = \pm \frac{\sqrt{6} \left( (6d - 4b)c^2 + bh(b-d)c - 2b^2 \right) \sqrt{c(bh-6c)(b-c^2)} - 6c(bh-6c)(b-c^2)}{c^2(bh-6c)^2},$$

$$x_k = \pm \frac{\sqrt{6} \sqrt{c(bh-6c)(b-c^2)}}{c(bh-6c)}, y_k = x_k - \frac{x_k^3}{3}.$$

Since the relationship between  $a_1$ ,  $a_2$ , and  $a_3$  can not be directly seen through the above expressions, a specific comparison will be given in the later numerical simulation.

Using the corresponding results in [8, 12, 24], we obtain the following theorem.

**Theorem 3.2.** *If the conditions  $a \neq -\frac{C}{B}$ ,  $-\frac{C-1}{B}$  hold and  $\tilde{a}(a_3) \neq 0$ , then model (1.3) undergoes a Neimark-Sacker bifurcation at  $E_k(x_k, y_k)$  when  $a = a_3$ . Moreover, the sign of  $\tilde{a}(a_3)$  decides the stability of bifurcating closed invariant curve. If  $\tilde{a}(a_3) < 0$  (resp.,  $\tilde{a}(a_3) > 0$ ), then the bifurcating closed invariant curve is attracting (resp., repelling) for  $a > a_3$  (resp.,  $a < a_3$ ).*

**Proof.** The following characteristic equation is given to analyze the local dynamics near the fixed points of the model (1.3):

$$\lambda^2 + p(a)\lambda + q(a) = 0,$$

where

$$p(a) = Ba + C, \quad q(a) = Da + E.$$

Then

$$|\lambda(a)| = \sqrt{Da + E},$$

$$l^* = \left. \frac{d|\lambda|}{da} \right|_{a=a_3} = \frac{D}{2}$$

$$= \frac{24c^3h^3x_k - (12bx_k + 18)c^2h^4}{(ch^2(2bx_k^2 - 3b + 3d + 6x_k) + h((4x_k^2 - 6)c^2 + 6b) + 12c)^2} \neq 0.$$

In addition,  $|\lambda(a_3)| = 1$ , and we require  $p(a_3) \neq 0, 1$ , which means

$$a_3 \neq -\frac{C}{B}, \quad -\frac{C-1}{B}$$

then  $\lambda^n(a_3) \neq 1$ ,  $n = 1, 2, 3, 4$ . There exist  $p_3, q_3 \in C^2$  such that

$$J(a_3, x_k, y_k)q_3 = \lambda(a_3)q_3, \quad J(a_3, x_k, y_k)\bar{q}_3 = \bar{\lambda}(a_3)\bar{q}_3$$

and

$$J^T(a_3, x_k, y_k)p_3 = \bar{\lambda}(a_3)p_3, \quad J^T(a_3, x_k, y_k)\bar{p}_3 = \lambda(a_3)\bar{p}_3.$$

After calculation,  $p, q$  can be chosen as

$$q_3 \sim (q_3^*, 1)^T, \quad p_3 \sim (p_3^*, 1)^T,$$

where

$$q_3^* = \frac{-\frac{1}{2}c(bhx_k - 2cx_k) + \frac{3}{2}h\sqrt{2}\sqrt{128}}{(ch^2(2bx_k^2 - 3b + 3d + 6x_k) + h((4x_k^2 - 6)c^2 + 6b) + 12c)^2} \\ \times \frac{\sqrt{c(hc^2(2x_k^2 - 3) + (6 + (bx_k^2 + \frac{3(d-b)}{2} + 3x_k)h^2)c + 3bh)^2(h(x_k^3 - \frac{3x_k}{2})c^2 + (\frac{3h^2x_k^2}{8} + 3x_k)c - \frac{9h}{4})}}{(ch^2(2bx_k^2 - 3b + 3d + 6x_k) + h((4x_k^2 - 6)c^2 + 6b) + 12c)^2(2bhx_k - 4cx_k + 3h)^2} \\ \times \frac{\sqrt{(\frac{9-3x_k^2-6dx_k}{2})c^2 + hc(bx_k^2 + \frac{3(d-b)}{2} + 3x_k)(bx_k + \frac{3}{2}) + 3b^2x_k + \frac{9b}{2}}}{(ch^2(2bx_k^2 - 3b + 3d + 6x_k) + h((4x_k^2 - 6)c^2 + 6b) + 12c)^2(2bhx_k - 4cx_k + 3h)^2} \\ + \frac{4c(h(2x_k^2 - 3)c^2 + (6 + (bx_k^2 - \frac{3}{2}b + \frac{3}{2}d + 3x_k)h^2)c + 3bh)c(h(bx_k^3 - \frac{3}{2}bx_k + \frac{9}{4}x_k^2 - \frac{9}{4})c + 3bx_k)}{(ch^2(2bx_k^2 - 3b + 3d + 6x_k) + h((4x_k^2 - 6)c^2 + 6b) + 12c)^2},$$

$$p_3^* = \frac{2\sqrt{2}(bx_k - 2cx_k + \frac{3}{2}h)\sqrt{128}}{24(-2cx_k + h(bx_k + \frac{3}{2})) (h(2x_k^2 - 3)c^2 + (6 + (bx_k^2 - \frac{3}{2}b + \frac{3}{2}d + 3x_k)h^2)c + 3bh)c^2} \\ \times \frac{\sqrt{c(hc^2(2x_k^2 - 3) + (6 + (bx_k^2 + \frac{3(d-b)}{2} + 3x_k)h^2)c + 3bh)^2(h(x_k^3 - \frac{3x_k}{2})c^2 + (\frac{3h^2x_k^2}{8} + 3x_k)c - \frac{9h}{4})}}{(24(-2cx_k + h(bx_k + \frac{3}{2})) (h(2x_k^2 - 3)c^2 + (6 + (bx_k^2 - \frac{3}{2}b + \frac{3}{2}d + 3x_k)h^2)c + 3bh)c^2) (2bhx_k - 4cx_k + 3h)^2} \\ \times \frac{(\frac{9-3x_k^2-6dx_k}{2})c^2 + hc(bx_k^2 + \frac{3(d-b)}{2} + 3x_k)(bx_k + \frac{3}{2}) + 3b^2x_k + \frac{9b}{2}}{(24(-2cx_k + h(bx_k + \frac{3}{2})) (h(2x_k^2 - 3)c^2 + (6 + (bx_k^2 - \frac{3}{2}b + \frac{3}{2}d + 3x_k)h^2)c + 3bh)c^2) (2bhx_k - 4cx_k + 3h)^2} \\ + \frac{16(h(2x_k^2 - 3)c^2 + (6 + (bx_k^2 - \frac{3}{2}b + \frac{3}{2}d + 3x_k)h^2)c + 3bh)c(h(bx_k^3 - \frac{3}{2}bx_k + \frac{9}{4}x_k^2 - \frac{9}{4})c + 3bx_k)}{24(-2cx_k + h(bx_k + \frac{3}{2})) (h(2x_k^2 - 3)c^2 + (6 + (bx_k^2 - \frac{3}{2}b + \frac{3}{2}d + 3x_k)h^2)c + 3bh)c^2}.$$

Normalizing  $p_3$  with respect to  $q_3$ , we have

$$q_3 = (q_3^*, 1)^T, \quad p_3 = \kappa_3(p_3^*, 1)^T,$$

where

$$\kappa_3 = \frac{1}{p_3^* q_3^* + 1}.$$

Through the transformations based on the theorems [12], the restriction of the model (3.1) to the center manifold takes the form

$$z \mapsto e^{i\theta(a_3)} z(1 + \tilde{d}(a_3)|z|^2) + O(|z|^4),$$

where  $e^{i\theta(a_3)} = \lambda(a_3)$ ,  $z \in C^2$  and the real number  $\tilde{d}(a_3) = \text{Re}(d(a_3))$  is given by the following formula:

$$\tilde{d}(a_3) = \frac{1}{2} \text{Re} \left\{ e^{-i\theta(a_3)} \left[ \langle p_3, C(q_3, q_3, \bar{q}_3) \rangle + 2 \langle p_3, B \left( q_3, (I_2 - J(a_3))^{-1} B(q_3, \bar{q}_3) \right) \rangle \right] \right. \\ \left. + \langle p_3, B \left( \bar{q}_3, (e^{2i\theta(a_3)} I_2 - J(a_3))^{-1} B(q_3, q_3) \right) \rangle \right\}.$$

□

## 4. Numerical simulations

The numerical simulations in this paper are realized by the software MATLAB R2020a. In the following cases, we consider different bifurcation parameters respectively. Case (i) chooses the parameter  $a$  and the step size  $h$  as the bifurcation parameter respectively. Case (ii) chooses  $a$  as the free parameter. In order to compare the NSFD scheme with the forward Euler scheme, the step size  $h$  is chosen as the free parameter to carry out bifurcation analysis of the model (1.2) and model (1.3) respectively in case (iii).

(i) When  $a = 1.080$ ,  $b = 5$ ,  $c = 1$ ,  $d = 2$  and  $h = 0.1$ , seen from Figure. 1(a), model (1.3) undergoes the fold bifurcation at the point  $(0.6, 0.528)$  with  $\tilde{a}(a_0) = -0.5127203730 < 0$ . So two fixed points bifurcated from  $(0.6, 0.528)$  for  $a < a_0$  which is illustrated by Theorem 3.1. Figure. 1(b) presents the bifurcation diagram which shows the bifurcating process for  $h \in (0, 1)$  and confirms that fold bifurcation is independent of the value of  $h$ .

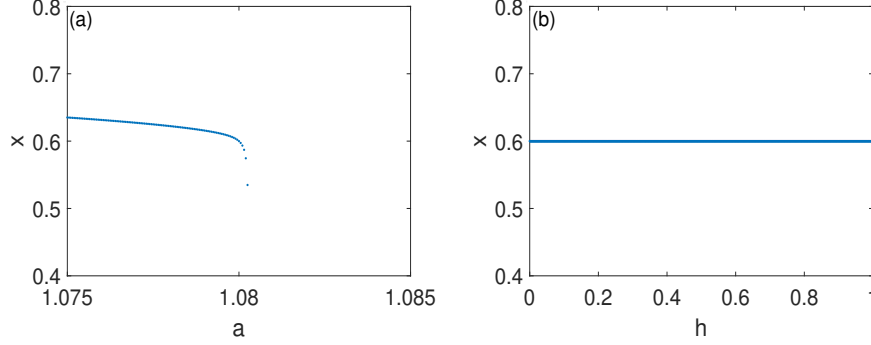


**Figure 1.** (a) Bifurcation diagram of model (1.3) in  $(a, x)$  plane for  $b = 5, c = 1, d = 2, h = 0.1$ , the initial condition is  $(0.6, 0.528)$ . (b) Bifurcation diagram of model (1.3) in  $(h, x)$  plane for  $a = 1.080, b = 5, c = 1, d = 2$ , the initial condition is  $(0.6, 0.528)$ .

(ii) When  $a = 1.202251732$ ,  $b = 1$ ,  $c = 2$ ,  $d = 3$ , and  $h = 0.1$ , there exists a unique fixed point  $(-0.8696565516, -0.6504154051)$  for model (1.3). When  $a \approx 1.202251732$ , the Neimark-Sacker bifurcation occurs at the point  $(-0.8696565516, -0.6504154051)$  and its eigenvalues are  $\lambda_{1,2} \approx 0.9947971165 \pm 0.1018758902i$ . For  $a = 1.202251732$ , there are  $|\lambda| = 1$ ,  $l^* = \frac{d|\lambda|}{da_3} = -0.0006179753 < 0$  and  $\tilde{d}(a_3) = -3.476537096 < 0$ . Fixed parameters  $h = 0.1, b = 1, c = 2, d = 3$ , model (1.2) undergoes the Neimark-Sacker bifurcation at  $(-0.8947368423, -0.6559751179)$  when  $a \approx 1.227681392$ . It is easy to compute that model (1.1) undergoes the Hopf bifurcation at  $(-0.8660254043, -0.6495190530)$  when  $a \approx 1.198557159$ . The error of bifurcation parameter  $a$  of the model (1.3) is  $e_1 = |a_3 - a_1| = 0.003694573$ , while the error of model (1.2) is  $e_2 = |a_2 - a_1| = 0.029124233 > 0.003694573$ . So we conclude that the Neimark-Sacker bifurcation of the model (1.3) is closer to model (1.1) than model (1.2). Figure. 2(a) presents the bifurcation diagrams which show the process of bifurcation and the occurrence of a closed invariant curve. Figure. 2(b) corresponds to the forward Euler method. We also plot the maximum Lyapunov exponents which show the emergence of periodic orbits and chaotic regions when the free parameter  $a$  changes in Figures. 2(c)-(d). Some typical phase portraits of the model (1.3) are also plotted in Figure. 4.

(iii) Corresponding to the conditions (ii), the step size  $h$  is chosen as the bifurcation parameter. Figures. 3(a)-(b) display the bifurcation diagrams which show the bifurcating process of the Neimark-Sacker bifurcation of the model (1.3) and model (1.2), respectively. The stability of the fixed points is illustrated by calculating the maximum Lyapunov exponents in Figures. 3(c)-(d) respectively corresponding to Figures. 3(a)-(b). To have a more intuitive comparison between the NSFD scheme and the forward Euler scheme, two-dimensional parameter-plane diagrams of the model (1.2) and model (1.3) are presented respectively in Figure. 3(e) and

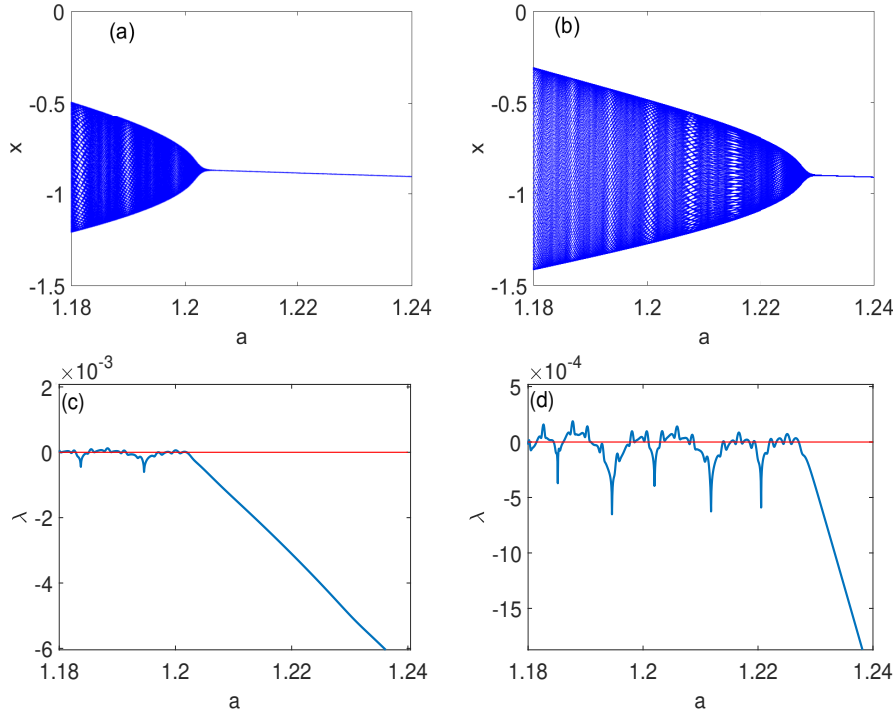


**Figure 2.** (a) Neimark-Sacker bifurcation diagram of model (1.3) in  $(a, x)$  plane for  $b = 1, c = 2, d = 3, h = 0.1$ , the initial condition is  $(-0.8, -0.6)$ . (b) Neimark-Sacker bifurcation diagram of model (1.2) in  $(a, x)$  plane for  $b = 1, c = 2, d = 3, h = 0.1$ , the initial condition is  $(-0.8, -0.6)$ . (c) Maximum Lyapunov exponents corresponding to (a). (d) Maximum Lyapunov exponents corresponding to (b).

Figure. 3(f), which shows the emergence of the chaotic phenomenon and periodic structure clearly. Comparing Figure. 3(e) with Figure. 3(f), within the same range, Figure. 3(f) has more overflow, which is due to the divergence of the forward Euler scheme. So we infer that applying the NSFD scheme to discretize a continuous-time system could get more results. Moreover, we can see more complex dynamic phenomena. As we see in Figure. 3(a), the fixed point undergoes the Neimark-Sacker bifurcation and is enclosed by a closed invariant cycle. When the step size  $h$  lies in a small neighborhood of 1.2299, the corresponding maximum Lyapunov exponents are positive, which implies the possibility of the occurrence of chaotic phenomena [18]. The occurrence of closed invariant curves and chaotic attractors are displayed in Figure. 5. Meanwhile, the variation between  $e_1 = |a_3 - a_1|$ ,  $e_2 = |a_2 - a_1|$  and the step size  $h$  is given in Table 1. As seen from Table 1, when  $h = 0.757785471$ ,  $e_1$  is approximately equal to the value of  $e_2$  with  $h = 0.1$ , which demonstrates the following conclusions:

1. Taking the same step size  $h$ , the error of the NSFD scheme  $e_1$  is smaller than the error of the forward Euler method  $e_2$ .
2. The step size  $h$  in the model (1.3) can be taken in a wide range.
3. The Hopf bifurcation of the model (1.3) obtained by the NSFD method is much closer to the original model (model (1.1)) than the model (1.2) obtained by the forward Euler method.

Furthermore, since model (1.1) is independent of  $h$  so that  $a_1$  is taken as  $a_1 =$

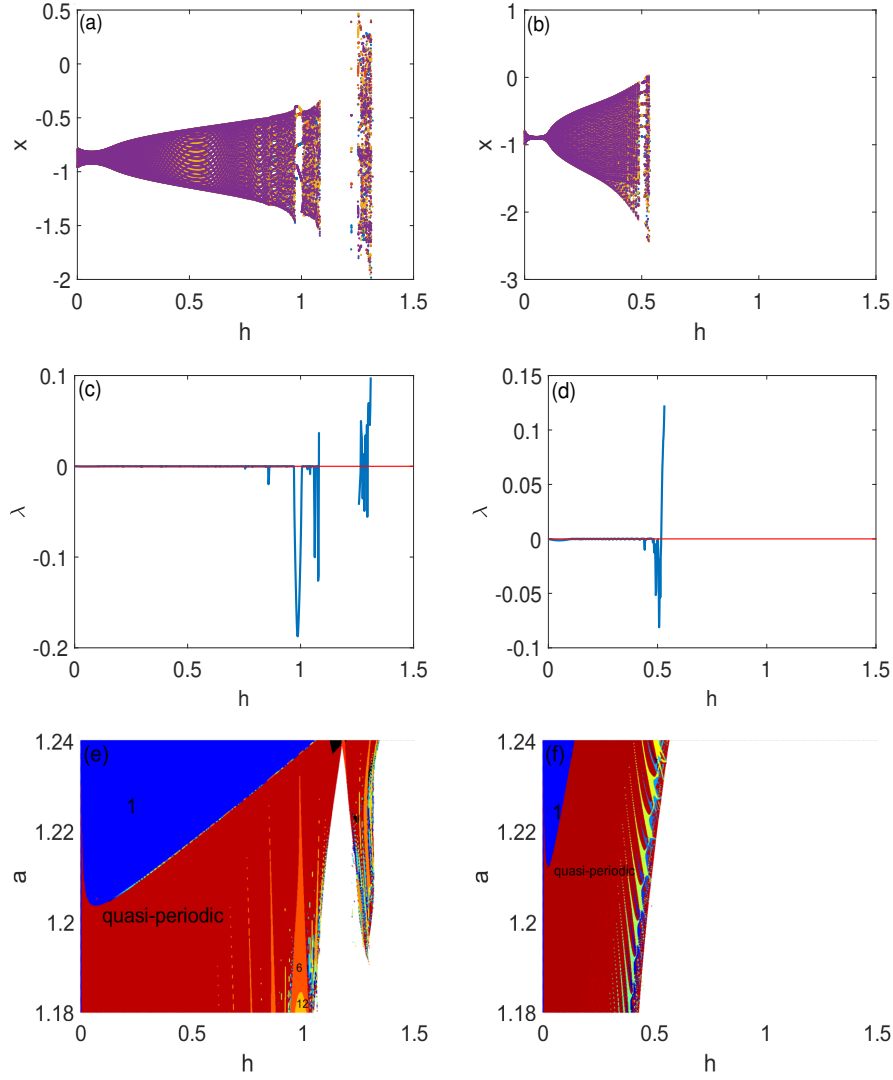


**Figure 3.** (a) Neimark-Sacker bifurcation diagram of model (1.3) in  $(h, x)$  plane for  $a = 1.2023, b = 1, c = 2, d = 3$ , the initial condition is  $(-0.8, -0.6)$ . (b) Neimark-Sacker bifurcation diagram of model (1.2) in  $(h, x)$  plane for  $a = 1.2277, b = 1, c = 2, d = 3$ , the initial condition is  $(-0.8, -0.6)$ . (c) Maximum Lyapunov exponents corresponding to (a). (d) Maximum Lyapunov exponents corresponding to (b). (e) Two-dimensional parameter-plane diagram in  $(h, a)$  plane corresponding to (a). (f) Two-dimensional parameter-plane diagram in  $(h, a)$  plane corresponding to (b).

1.198557159 in Table 1. From Table 1, it is clear that as  $h \rightarrow 0$ , the critical values of bifurcation parameter  $a$  for the emergence of Hopf bifurcation and Neimark-Sacker bifurcation are nearly identical, that is,  $e_1 = |a_3 - a_1| \rightarrow 0$ .

## 5. Conclusions

In this paper, a discrete-time Hindmarsh-Rose model is obtained by the NSFD scheme in  $R^2$ . Fortunately, its explicit expression can be solved, which facilitates

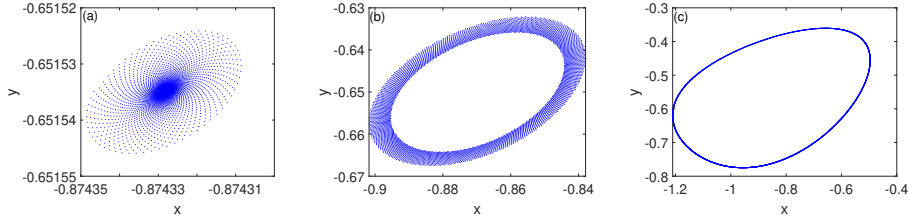


**Figure 4.** Phase portraits for various values of  $a$  corresponding to Figure. 2(a). (a) Orbits for  $a = 1.207$ . (b) Orbits for  $a = 1.20235$ . (c) An invariant cycle for  $a = 1.18$ .

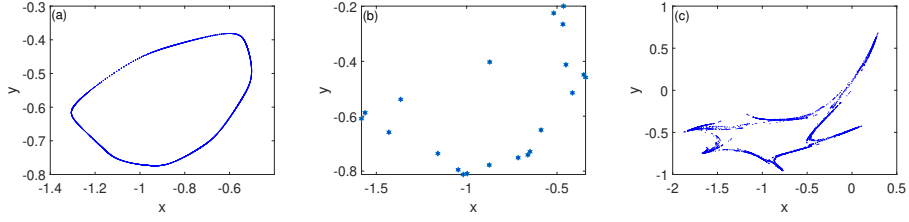


**Figure 5.** Phase portraits for various values of  $h$  corresponding to Figure. 3(a). (a) An invariant cycle for  $h = 0.855$ . (b) Period-21 orbits for  $h = 1.081$ . (c) A chaotic attractor for  $h = 1.299$ , and the corresponding Maximum Lyapunov exponents is about equal to 0.06967.

**Table 1.** Variation of  $a_3$ ,  $|a_3 - a_1|$  and  $a_2$ ,  $|a_2 - a_1|$  with different values of  $h$ .

$h$	$a_3$	$e_1 =  a_3 - a_1 $	$a_2$	$e_2 =  a_2 - a_1 $
0.0000001	1.198557163	$4 \times 10^{-9}$	1.198557188	$2.9 \times 10^{-8}$
0.00001	1.198557526	$3.67 \times 10^{-7}$	1.198560149	$2.99 \times 10^{-6}$
0.001	1.198593893	0.000036734	1.198856204	0.000299045
0.1	1.202251732	0.003694573	1.227681392	0.029124233
0.3	1.209771941	0.011214782	1.282178621	0.083621462
0.5	1.217473491	0.018916332	1.333333333	0.134776174
0.7	1.225364787	0.026807628	1.382585944	0.184028785
0.757785471	1.227681393	0.029124234	1.396623222	0.198066063

our research. The fold bifurcation and the Neimark-Sacker bifurcation have been investigated by using the center manifold theorem and bifurcation theory.

Compared with the forward Euler scheme, our investigation demonstrates that the difference equation obtained by the NSFD scheme is closer to the original continuous system. The convergence and stability of the NSFD scheme are much better than the forward Euler scheme, which has been demonstrated by comparing the relevant properties between model (1.2) and model (1.3). When the step size  $h$  increases, the forward Euler method diverges earlier than the NSFD method, which makes the model (1.3) obtained by the NSFD method get more dynamic behaviors. Moreover, taking the Hopf bifurcation as an example, with the same step size  $h$ , the bifurcation parameter of the model (1.3) is closer to the original continuous model than the model (1.2). Therefore, it is much better to use the NSFD scheme to discretize continuous systems than the forward Euler scheme from the perspective of retaining the structure of the original system as much as possible.

Due to the complexity of this Hindmarsh-Rose model, it is hard to obtain the

direct relationship of the eigenvalues of the Jacobian matrices between the differential equations and the resulting difference equations in a strictly theoretical way. So it limits the strict theoretical deduction concerning the comparison between the differential equations and the resulting difference equations in depth. Therefore, what we can do depends on mostly the bifurcation analysis and numerical simulations, respectively. Even so, it is worthwhile to take into account these comparisons between the NSFD scheme and the forward Euler scheme. This is because through these comparisons, on the one hand, we can build up much more experience to deal with a similar problem. On the other hand, these confirmed methods can guarantee the accuracy of numerical results for complex neuron dynamical systems.

## Appendix A

A NSFD scheme is applied to the model (1.1) as shown in the following formula:

$$\begin{cases} \frac{x_{n+1} - x_n}{h} = \frac{c(x_n + x_{n+1})}{2} - \frac{cx_n^2 x_{n+1}}{3} - \frac{c(y_n + y_{n+1})}{2}, \\ \frac{y_{n+1} - y_n}{h} = \frac{x_n x_{n+1} + \frac{d(x_n + x_{n+1})}{2} - \frac{b(y_n + y_{n+1})}{2} + a}{c}, \end{cases}$$

where  $h > 0$  is the step size and the approximations  $x_n \mapsto \frac{x_n + x_{n+1}}{2}$ ,  $x_n^2 \mapsto x_n x_{n+1}$ ,  $x_n^3 \mapsto x_n^2 x_{n+1}$  and  $y_n \mapsto \frac{y_n + y_{n+1}}{2}$  are used to approximate  $x_n$ ,  $x_n^2$ ,  $x_n^3$  and  $y_n$  terms.

Notice that  $x_{n+1}$  and  $y_{n+1}$  in the above formula can be solved. Writing the discrete system in the form of mapping, the model (1.3) is obtained.

## Appendix B

$$\begin{aligned} J_{11} &= \frac{-24(x_k^2 - 4x_k y_k + \frac{3}{2})h^2 c^4 + 48h \left( \left( (-\frac{1}{2}x_k^2 + x_k y_k - \frac{3}{4})b + \frac{dx_k^2}{4} + ax_k + \frac{3d}{4} + \frac{3y_k}{2} \right) h^2 - x_k^2 \right) c^3}{M^2(k)} \\ &\quad + \frac{(144 + ((-6x_k^2 - 9)b^2 + (6dx_k^2 + 24ax_k + 18d)b - 9d^2 + 36a)h^4 - 48bh^2 x_k^2) c^2}{M^2(k)} \\ &\quad + \frac{(-12b^2 h^3 x_k^2 + 144bh)c + 36b^2 h^2}{M^2(k)}, \\ J_{12} &= \frac{-12c^2 h}{M(k)}, \\ J_{21} &= -\frac{12ch^2 \left( \left( -\frac{dx_k^4}{9} + \left( \frac{d}{2} - \frac{2y_k}{3} \right) x_k^2 + \left( 1 - \frac{2dy_k}{3} \right) x_k - y_k \right) c^2 - \left( \frac{db}{6} + 1 \right) x_k^2 - dx_k + \frac{db}{2} - \frac{d^2}{2} + a \right)}{M^2(k)} \\ &\quad - \frac{24h^3 \left( c^2 \left( \frac{bdx_k^4}{6} + dx_k^3 + a + \frac{3}{2} - \frac{3}{4}db \right) x_k^2 + \left( \left( a + \frac{3}{2} \right) d - \frac{3b}{2} \right) x_k + \frac{3a}{2} \right)}{M^2(k)} \\ &\quad + \frac{4h \left( (dx_k^2 - 3d - 6y_k) c^2 + 3b(d + 2x_k) \right) h + 6c(d + 2x_k)}{M^2(k)}, \\ J_{22} &= \frac{h(4x_k^2 - 6)c^2 + (12 - (2bx_k^2 - 3b + 3d + 6x_k)h^2)c - 6bh}{M(k)}, \end{aligned}$$

## Appendix C

$$\begin{aligned}
B &= \frac{(24bx_k + 36)c^2h^4 + 48c^3x_kh^3}{M^2(k)}, \\
C &= \frac{-4c^2h^4 \left( b^2x_k^4 + 6bx_k^3 + \left(-\frac{3}{2}b^2 + 9 + \frac{3}{2}bd\right)x_k^2 + 9(d-b)x_k + \frac{9(b-d)^2}{2} \right)}{M^2(k)} \\
&\quad + \frac{4ch^3 \left( ((6b-3d)x_k^2 - 12bx_ky_k + 9b - 9d - 18y_k)c^2 + 9b(bx_k^2 - b + d + 2x_k) \right)}{M^2(k)} \\
&\quad + \frac{12 \left( \left(-\frac{1}{3}x_k^3 + \frac{3}{2}x_k - 2y_k\right)c^2 + bx_k \right) x_k c^2 h^2 + \left( (36 - 12x^2)c^2 - 36b \right) ch - 72c^2}{M^2(k)}, \\
D &= \frac{48c^3x_kh^3 - (24bx_k + 36)c^2h^4}{M^2(k)}, \\
E &= \frac{-24h^2c^4 \left( x_k^2 - 4x_ky_k + \frac{3}{2} \right) - 48hc^3 \left( \left(-\frac{3dx_k^2}{4} + (by_k - \frac{3}{2})x_k + \frac{3y_k}{2} \right) h^2 + x_k^2 \right)}{M^2(k)} \\
&\quad + \frac{(144 + 6(b-d)(x_k^2 + \frac{3}{2}(b-d))h^4 + (72d + 144x_k)h^2)c^2 + 12b^2ch^3x_k^2 - 36b^2h^2}{M^2(k)}.
\end{aligned}$$

**Remark.**  $M(k)$  is equal to the value of  $M$  at  $x = x_k$ .

## Appendix D

The proofs of **Proposition 2.1** and **Proposition 2.2** are as follow:

**Proof.** 1.  $\Delta < 0$ :

When  $\Delta < 0$ , that is  $\frac{-BC+2D-2\sqrt{B^2E-BCD+D^2}}{B^2} < a < \frac{-BC+2D+2\sqrt{B^2E-BCD+D^2}}{B^2}$ , then there exist two pairs of conjugate complex eigenvalues of model (3) as follows:

$$\lambda_{1,2} = \frac{1}{2} \left( Ba + C \pm i\sqrt{4(Da + E) - (Ba + C)^2} \right).$$

The modules of these eigenvalues at the fixed point  $E_k$  are easily calculated and found to be  $|\lambda_{1,2}| = \sqrt{Da + E}$ . Next, the following two cases should be considered.

Case 1: The fixed point  $E_k$  is a stable focus if  $|\lambda_{1,2}| < 1$ , i.e., the following conditions are satisfied:

$$\begin{cases} \Delta < 0, \\ |\lambda_{1,2}| < 1. \end{cases} \Rightarrow \begin{cases} \frac{-BC+2D-2\sqrt{B^2E-BCD+D^2}}{B^2} < a < \frac{-BC+2D+2\sqrt{B^2E-BCD+D^2}}{B^2}, \\ a < \frac{1-E}{D} (D > 0); \quad a > \frac{1-E}{D} (D < 0). \end{cases} \quad (5.1)$$

From the inequalities (5.1), we obtain

$$\begin{aligned}
&\frac{-BC+2D-2\sqrt{B^2E-BCD+D^2}}{B^2} < a < \frac{-BC+2D+2\sqrt{B^2E-BCD+D^2}}{B^2}, a < \frac{1-E}{D} (D > 0) \\
\text{or } &\frac{-BC+2D-2\sqrt{B^2E-BCD+D^2}}{B^2} < a < \frac{-BC+2D+2\sqrt{B^2E-BCD+D^2}}{B^2}, a > \frac{1-E}{D} (D < 0).
\end{aligned}$$

Case 2: The fixed point  $E_k$  is an unstable focus if  $|\lambda_{1,2}| > 1$ , i.e., the following conditions are satisfied:

$$\begin{cases} \Delta < 0, \\ |\lambda_{1,2}| > 1. \end{cases} \Rightarrow \begin{cases} \frac{-BC+2D-2\sqrt{B^2E-BCD+D^2}}{B^2} < a < \frac{-BC+2D+2\sqrt{B^2E-BCD+D^2}}{B^2}, \\ a > \frac{1-E}{D} (D > 0); \quad a < \frac{1-E}{D} (D < 0). \end{cases} \quad (5.2)$$

From the inequalities (5.2), we obtain

$$\begin{aligned} & \frac{-BC+2D-2\sqrt{B^2E-BCD+D^2}}{B^2} < a < \frac{-BC+2D+2\sqrt{B^2E-BCD+D^2}}{B^2}, \quad a > \frac{1-E}{D} (D > 0) \\ \text{or } & \frac{-BC+2D-2\sqrt{B^2E-BCD+D^2}}{B^2} < a < \frac{-BC+2D+2\sqrt{B^2E-BCD+D^2}}{B^2}, \quad a < \frac{1-E}{D} (D < 0). \end{aligned}$$

2.  $\Delta \geq 0$ :

When  $\Delta \geq 0$ , that is  $a \geq \frac{2D-BC+2\sqrt{B^2E-BCD+D^2}}{B^2}$  or  $a \leq \frac{2D-BC-2\sqrt{B^2E-BCD+D^2}}{B^2}$ , then there exist two different real eigenvalues of model (3) as follows:

$$\lambda_{1,2} = \frac{1}{2} \left( Ba + C \pm \sqrt{(Ba + C)^2 - 4(Da + E)} \right).$$

There are three cases depending on the modules of  $|\lambda_{1,2}|$ .

Case 1: The fixed point  $E_k$  is a stable sink if  $|\lambda_{1,2}| < 1$ , i.e., the following conditions are satisfied:

$$\begin{cases} \Delta \geq 0, \\ h(1) > 0, \\ h(-1) > 0, \\ -2 < \lambda_1 + \lambda_2 < 2, \\ -1 < \lambda_1 \lambda_2 < 1. \end{cases} \Rightarrow \begin{cases} a \geq \frac{2D-BC+2\sqrt{B^2E-BCD+D^2}}{B^2} \text{ or } a \leq \frac{2D-BC-2\sqrt{B^2E-BCD+D^2}}{B^2}, \\ a < \frac{1+E-C}{B-D} (B-D > 0); \quad a > \frac{1+E-C}{B-D} (B-D < 0), \\ a < \frac{-1-E-C}{B+D} (B+D < 0); \quad a > \frac{-1-E-C}{B+D} (B+D > 0), \\ \frac{-C-2}{B} < a < \frac{-C+2}{B} (B > 0); \quad \frac{-C+2}{B} < a < \frac{-C-2}{B} (B < 0), \\ -1 < Da + E < 1. \end{cases} \quad (5.3)$$

It is easy to calculate that there is no solution to the inequalities (5.3).

Case 2: The fixed point  $E_k$  is an unstable source if  $|\lambda_{1,2}| > 1$ , i.e., the following conditions are satisfied:

$$\begin{cases} \Delta \geq 0, \\ h(1) > 0, \\ h(-1) < 0. \end{cases} \Rightarrow \begin{cases} a \geq \frac{2D-BC+2\sqrt{B^2E-BCD+D^2}}{B^2} \text{ or } a \leq \frac{2D-BC-2\sqrt{B^2E-BCD+D^2}}{B^2}, \\ a < \frac{1+E-C}{B-D} (B-D < 0); \quad a > \frac{1+E-C}{B-D} (B-D > 0), \\ a < \frac{-1-E-C}{B+D} (B+D > 0); \quad a > \frac{-1-E-C}{B+D} (B+D < 0). \end{cases} \quad (5.4)$$

or

$$\begin{cases} \Delta \geq 0, \\ \frac{Ba+C}{2} < -1, \\ h(-1) > 0. \end{cases} \Rightarrow \begin{cases} a \geq \frac{2D-BC+2\sqrt{B^2E-BCD+D^2}}{B^2} \text{ or } a \leq \frac{2D-BC-2\sqrt{B^2E-BCD+D^2}}{B^2}, \\ a < -\frac{C+2}{B} (B > 0); \quad a > -\frac{C+2}{B} (B < 0), \\ a < \frac{-1-E-C}{B+D} (B+D < 0); \quad a > \frac{-1-E-C}{B+D} (B+D > 0). \end{cases} \quad (5.5)$$

or

$$\left\{ \begin{array}{l} \Delta \geq 0, \\ \frac{Ba+C}{2} > 1, \\ h(1) > 0. \end{array} \right. \Rightarrow \left\{ \begin{array}{l} a \geq \frac{2D-BC+2\sqrt{B^2E-BCD+D^2}}{B^2} \text{ or } a \leq \frac{2D-BC-2\sqrt{B^2E-BCD+D^2}}{B^2}, \\ a > \frac{-C+2}{B} (B > 0); \ a > \frac{-C+2}{B} (B < 0), \\ a < \frac{1+E-C}{B-D} (B-D > 0); \ a > \frac{1+E-C}{B-D} (B-D < 0). \end{array} \right. \quad (5.6)$$

Case 3: The fixed point  $E_k$  is a saddle if  $|\lambda_1| < 1, |\lambda_2| > 1$ , or  $|\lambda_1| > 1, |\lambda_2| < 1$ , i.e., the following conditions are satisfied:

$$\left\{ \begin{array}{l} \Delta > 0, \\ h(-1)h(1) < 0. \end{array} \right. \Rightarrow \left\{ \begin{array}{l} a \geq \frac{2D-BC+2\sqrt{B^2E-BCD+D^2}}{B^2} \text{ or } a \leq \frac{2D-BC-2\sqrt{B^2E-BCD+D^2}}{B^2}, \\ \frac{D-BC+\sqrt{(E+1)^2B^2-2BCD+D^2}(C^2-E^2-2E)}{B^2-D^2} < a < \frac{D-BC-\sqrt{(E+1)^2B^2-2BCD+D^2}(C^2-E^2-2E)}{B^2-D^2} \\ (D^2 - B^2 > 0); \\ a < \frac{D-BC-\sqrt{(E+1)^2B^2-2BCD+D^2}(C^2-E^2-2E)}{B^2-D^2} \\ \text{or } a > \frac{D-BC+\sqrt{(E+1)^2B^2-2BCD+D^2}(C^2-E^2-2E)}{B^2-D^2} \\ (D^2 - B^2 < 0). \end{array} \right. \quad (5.7) \quad \square$$

## Appendix E

$$\begin{aligned} b_1 &= -\frac{2(6hc^2 + ((3b-3d)h^2 + 12)c + 6bh)(-8hc^2x_k + (-4bx_k + 6)h^2c)}{(4h(-\frac{3}{2} + x_k^2)c^2 + (12 + (2bx_k^2 - 3b + 3d - 6x_k)h^2)c + 6bh)^2} \\ &\quad - \frac{(6h(-x_k + 2y_k)c^2 + ((3d-3b)x_k - 6a)h^2 - 12x_k)c - 6bhx_k(4bch^2 + 8hc^2)}{(4h(-\frac{3}{2} + x_k^2)c^2 + (12 + (2bx_k^2 - 3b + 3d - 6x_k)h^2)c + 6bh)^2} \\ &\quad + \frac{2(6h(-x_k + 2y_k)c^2 + ((3d-3b)x_k - 6a)h^2 - 12x_k)c - 6bhx_k(-8hc^2x_k + (-4bx_k + 6)h^2c)^2}{(4h(-\frac{3}{2} + x_k^2)c^2 + (12 + (2bx_k^2 - 3b + 3d - 6x_k)h^2)c + 6bh)^3}, \\ b_2 &= \frac{4c(by_k - 3dx_k + 2a + 3)h^2 + (-8c^2y_k + 24)h}{c(2bx_k^2 - 3b + 3d - 6x_k)h^2 + ((4x_k^2 - 6)c^2 + 6b)h + 12c} \\ &\quad - \frac{(8c(\frac{3(y_k + dx_k^2)}{2} - 2x_k(a + \frac{by_k + 3}{2})))h^2 + 8(2c^2x_ky_k + 3d - 6x_k)h)((6 - 4bx_k)h^2c - 8hx_kc^2)}{(c(2bx_k^2 - 3b + 3d - 6x_k)h^2 + ((4x_k^2 - 6)c^2 + 6b)h + 12c)^2} \\ &\quad + \frac{2(ch^2(4x_k^2(a + \frac{by_k + 3}{2}) - 6(x_ky_k + a) - dx_k^3 - 3y_k(b-a)) + (12(a + x_k^2) + c^2y_k(6 - 4x_k^2) + 6by_k - 12dx_k)h - 12cy_k)}{(c(2bx_k^2 - 3b + 3d - 6x_k)h^2 + ((4x_k^2 - 6)c^2 + 6b)h + 12c)^2} \\ &\quad \times \frac{((6 - 4bx_k)h^2c - 8hx_kc^2)^2}{(c(2bx_k^2 - 3b + 3d - 6x_k)h^2 + ((4x_k^2 - 6)c^2 + 6b)h + 12c)^3} \\ &\quad - \frac{(ch^2(4x_k^2(a + \frac{by_k + 3}{2}) - 6(x_ky_k + a) - dx_k^3 - 3y_k(b-a)) + (12(a + x_k^2) + c^2y_k(6 - 4x_k^2) + 6by_k - 12dx_k)h - 12cy_k)}{(c(2bx_k^2 - 3b + 3d - 6x_k)h^2 + ((4x_k^2 - 6)c^2 + 6b)h + 12c)^2} \\ &\quad \times \frac{4(bch^2 + 2hc^2)}{(c(2bx_k^2 - 3b + 3d - 6x_k)h^2 + ((4x_k^2 - 6)c^2 + 6b)h + 12c)^2}, \\ b_3 &= \frac{12hc^2(-8hx_kc^2 + (-4bx_k + 6)h^2c)}{(4h(-\frac{3}{2} + x_k^2)c^2 + (12 + (2bx_k^2 - 3b + 3d - 6x_k)h^2)c + 6bh)^2}, \end{aligned}$$

$$\begin{aligned}
b_4 &= \frac{4(ch^2(bx_k - \frac{3}{2}) - 2hx_k c^2)}{c(2bx_k^2 - 3b + 3d - 6x_k)h^2 + ((4x_k^2 - 6)c^2 + 6b)h + 12c} \\
&\quad - \frac{(ch^2(6x_k - 2bx_k^2 + 3(b-d)) + ((4x_k^2 - 6)c^2 - 6b)h + 12c)((6-4bx_k)h^2 c - 8hx_k c^2)}{(c(2bx_k^2 - 3b + 3d - 6x_k)h^2 + ((4x_k^2 - 6)c^2 + 6b)h + 12c)^2}, \\
c_1 &= \frac{6(6hc^2 + ((3b-3d)h^2 + 12)c + 6bh)((6-4bx_k)h^2 c - 8hx_k c^2)^2}{(4hc^2(x_k^2 - \frac{3}{2}) + (12 + (2bx_k^2 - 3b + 3d - 6x_k)h^2)c + 6bh)^3} \\
&\quad - \frac{12(6hc^2 + ((3b-3d)h^2 + 12)c + 6bh)(bch^2 + 2hc^2)}{(4hc^2(x_k^2 - \frac{3}{2}) + (12 + (2bx_k^2 - 3b + 3d - 6x_k)h^2)c + 6bh)^2} \\
&\quad - \frac{6(6h(-x_k + 2y_k)c^2 + ((3d-3b)x_k - 6a)h^2 - 12x_k)c - 6bhx_k(-8hc^2 + (-4bx_k + 6)h^2 c)^3}{(4h(-\frac{3}{2} + x_k^2)c^2 + (12 + (2bx_k^2 - 3b + 3d - 6x_k)h^2)c + 6bh)^4} \\
&\quad - \frac{6(6h(-x_k + 2y_k)c^2 + ((3d-3b)x_k - 6a)h^2 - 12x_k)c - 6bhx_k(-8hc^2 x_k + (-4bx_k + 6)h^2 c)(4bch^2 + 8hc^2)}{(4h(-\frac{3}{2} + x_k^2)c^2 + (12 + (2bx_k^2 - 3b + 3d - 6x_k)h^2)c + 6bh)^3}, \\
c_2 &= \frac{12cdh^2}{ch^2(2bx_k^2 - 3b + 3d - 6x_k) + ((4x_k^2 - 6)c^2 + 6b)h + 12c} \\
&\quad - \frac{3(4c(by_k - 3dx_k + 2a + 3)h^2 + (24 - 8c^2 y_k)h)((6-4bx_k)h^2 c - 8hx_k c^2)}{(ch^2(2bx_k^2 - 3b + 3d - 6x_k) + ((4x_k^2 - 6)c^2 + 6b)h + 12c)^2} \\
&\quad + \frac{6(4c(-2x_k(a + \frac{by_k}{2} + \frac{3}{2}) + \frac{3y_k}{2} + \frac{3dx_k^2}{2})h^2 + (8c^2 x_k y_k + 12d - 24x_k)h)(-8hc^2 x_k + (-4bx_k + 6)h^2 c)^2}{(c(2bx_k^2 - 3b + 3d - 6x_k)h^2 + ((4x_k^2 - 6)c^2 + 6b)h + 12c)^3} \\
&\quad + \frac{3(4c(-2x_k(a + \frac{by_k}{2} + \frac{3}{2}) + \frac{3y_k}{2} + \frac{3dx_k^2}{2})h^2 + (8c^2 x_k y_k + 12d - 24x_k)h)(4bch^2 + 8hc^2)}{(c(2bx_k^2 - 3b + 3d - 6x_k)h^2 + ((4x_k^2 - 6)c^2 + 6b)h + 12c)^2} \\
&\quad - \frac{6(4ch^2(x_k^2(a + \frac{by_k + 3}{2}) - \frac{3(x_k y_k + a + dx_k^2)}{2}) - \frac{3y_k(b-1)}{4}) + (12(a+x_k^2) + c^2(6y-4x^2 y) + 6by_k - 12dx_k)h - 12cy)}{(c(2bx_k^2 - 3b + 3d - 6x_k)h^2 + ((4x_k^2 - 6)c^2 + 6b)h + 12c)^4} \\
&\quad \times \frac{((6-4bx_k)h^2 c - 8hx_k c^2)^3}{(c(2bx_k^2 - 3b + 3d - 6x_k)h^2 + ((4x_k^2 - 6)c^2 + 6b)h + 12c)^4} \\
&\quad + \frac{6(4ch^2(x_k^2(a + \frac{by_k + 3}{2}) - \frac{3(x_k y_k + a + dx_k^2)}{2}) - \frac{3y_k(b-1)}{4}) + (12(a+x_k^2) + c^2 y_k(6-4x_k^2) + 6by_k - 12dx_k)h - 12cy_k}{(c(2bx_k^2 - 3b + 3d - 6x_k)h^2 + ((4x_k^2 - 6)c^2 + 6b)h + 12c)^3} \\
&\quad \times \frac{((6-4bx_k)h^2 c - 8hx_k c^2)(4bch^2 + 8hc^2)}{(c(2bx_k^2 - 3b + 3d - 6x_k)h^2 + ((4x_k^2 - 6)c^2 + 6b)h + 12c)^3}, \\
c_3 &= -\frac{24hc^2(-8hx_k c^2 + (-4bx_k + 6)h^2 c)^2}{(4h(-\frac{3}{2} + x_k^2)c^2 + (12 + (2bx_k^2 - 3b + 3d - 6x_k)h^2)c + 6bh)^3} \\
&\quad + \frac{12hc^2(4bch^2 + 8hc^2)}{(4h(-\frac{3}{2} + x_k^2)c^2 + (12 + (2bx_k^2 - 3b + 3d - 6x_k)h^2)c + 6bh)^2}, \\
c_4 &= \frac{4(-bch^2 + 2hc^2)}{ch^2(2bx_k^2 - 3b + 3d - 6x_k) + ((4x_k^2 - 6)c^2 + 6b)h + 12c} \\
&\quad - \frac{2(4ch^2(bx_k - \frac{3}{2}) - 8hx_k c^2)((6-4bx_k)h^2 c - 8hx_k c^2)}{(ch^2(2bx_k^2 - 3b + 3d - 6x_k) + ((4x_k^2 - 6)c^2 + 6b)h + 12c)^2} \\
&\quad + \frac{2(4c(-\frac{1}{2}bx_k^2 + \frac{3}{2}x_k + \frac{3}{4}b - \frac{3}{4}d)h^2 + ((4x_k^2 - 6)c^2 - 6b)h + 12c)(-8hx_k c^2 + (-4bx_k + 6)h^2 c)^2}{(c(2bx_k^2 - 3b + 3d - 6x_k)h^2 + ((4x_k^2 - 6)c^2 + 6b)h + 12c)^3} \\
&\quad - \frac{(4c(-\frac{1}{2}bx_k^2 + \frac{3}{2}x_k + \frac{3}{4}b - \frac{3}{4}d)h^2 + ((4x_k^2 - 6)c^2 - 6b)h + 12c)(4bch^2 + 8hc^2)}{(c(2bx_k^2 - 3b + 3d - 6x_k)h^2 + ((4x_k^2 - 6)c^2 + 6b)h + 12c)^2}.
\end{aligned}$$

## References

- [1] E. M. Adamu, K. C. Patidar and A. Ramanantoanina, *An unconditionally stable nonstandard finite difference method to solve a mathematical model describing Visceral Leishmaniasis*, Math. Comput. Simul., 2021, 187(12), 171–190.
- [2] H. Al-Kahby, F. Dannan and S. Elaydi, *Non-standard Discretization Methods for Some Biological Models*, World Scientific, Singapore, 2000.
- [3] M. Biswas and N. Bairagi, *On the dynamic consistency of a two-species competitive discrete system with toxicity: Local and global analysis*, J. Comput. Appl. Math., 2020, 363, 145–155.
- [4] S. Chen, C. Cheng and Y. Lin, *Application of a two-dimensional hindmarsh-*

- rose type model for bifurcation analysis*, Int. J. Bifurcation Chaos, 2013, 23(3), 50055.
- [5] Q. A. Dang and M. T. Hoang, *Numerical dynamics of nonstandard finite difference schemes for a computer virus propagation model*, Int. J. Dyn. Control., 2020, 8(3), 772–778.
- [6] D. T. Dimitrov and H. V. Kojouharov, *Nonstandard finite-difference methods for predator-prey models with general functional response*, Math. Comput. Simul., 2008, 78(1), 1–11.
- [7] C. C. Felicio and P. C. Rech, *Arnold tongues and the Devil's staircase in a discrete-time Hindmarsh-Rose neuron model*, Phys. Lett. A., 2015, 379(43–44), 2845–2847.
- [8] J. Guckenheimer and P. Holmes, *Nonlinear oscillations, dynamical systems, and bifurcations of vector fields*, Springer, New York, 1983.
- [9] W. Kahan and R. Li, *Unconventional Schemes for a Class of Ordinary Differential Equations-With Applications to the Korteweg-de Vries Equation*, J. Comput. Phys., 1997, 134(2), 316–331.
- [10] V. A. Kumar, R. M. Kumar and C. Carlo, *A numerical scheme for a class of generalized Burgers' equation based on Haar wavelet nonstandard finite difference method*, Appl. Numerical Math., 2021, 168, 41–54.
- [11] A. P. Kuznetsov and Y. V. Sedova, *The simplest map with three-frequency quasi-periodicity and quasi-periodic bifurcations*, Int. J. Bifurcation Chaos, 2016, 26(8), 1630019.
- [12] Y. A. Kuznetsov, *Elements of applied bifurcation theory, Second Edition*, Springer, New York, 1999.
- [13] B. Li and Q. He, *Bifurcation analysis of a two-dimensional discrete Hindmarsh-Rose type model*, Adv. Differ. Equ., 2019, 2019(1), 1–17.
- [14] B. Li and Z. He, *Bifurcations and chaos in a two-dimensional discrete Hindmarsh-Rose model*, Nonlinear Dyn., 2014, 76(1), 697–715.
- [15] R. E. Mickens, *Nonstandard Finite Difference Models of Differential Equations*, World Scientific, Singapore, 1993.
- [16] S. M. Moghadas, M. E. Alexander and B. D. Corbett, *A non-standard numerical scheme for a generalized Gause-type predator-prey model*, Phys. D., 2004, 188(1), 134–151.
- [17] M. Namjoo, M. Zeinadini and S. Zibaei, *Nonstandard finite-difference scheme to approximate the generalized Burgers-Fisher equation*, Math. Meth. Appl. Sci., 2018, 41(17), 8212–8228.
- [18] E. Ott, *Chaos in dynamical systems*, Cambridge University Press, Cambridge, UK, 1993.
- [19] L. I. W. Roeger, *Nonstandard finite-difference schemes for the Lotka-Volterra systems: generalization of Mickens's method*, J. Differ. Equ. Appl., 2006, 12(9), 937–948.
- [20] L. I. W. Roeger and G. Lahodny, *Dynamically consistent discrete Lotka-Volterra competition systems*, J. Differ. Equ. Appl., 2013, 19(2), 191–200.

- 
- [21] L. I. W. Roeger, *Local Stability of Euler's and Kahan's Methods*, J. Differ. Equ. Appl., 2004, 10(6), 601–614.
  - [22] S. Tsuji, T. Ueta, H. Kawakami, H. Fujii and K. Aihara, *Bifurcations in two-dimensional Hindmarsh-Rose type model*, Int. J. Bifurcation Chaos, 2007, 17(3), 985–998.
  - [23] H. Wang, Y. Zheng and Q. Lu, *Stability and bifurcation analysis in the coupled HR neurons with delayed synaptic connection*, Nonlinear Dyn., 2017, 88(3), 2091–2100.
  - [24] S. Wiggins, *Introduction to applied nonlinear dynamical systems and chaos*, Springer, New York, 1990.
  - [25] Y. Yu and H. Cao, *Integral step size makes a difference to bifurcations of a discrete-time Hindmarsh-Rose model*, Int. J. Bifurcation Chaos, 2015, 25(2), 1550029.